Harnessing defective interfering particles and lipid nanoparticles for effective delivery of an anti-dengue virus RNA therapy

Min-Hsuan Lin[1#], Pramila Maniam[1#], Dongsheng Li[1], Bing Tang[1], Cameron Bishop[1], Andreas Suhrbier[1,2], Lucy Wales- Earl[3], Yaman Tayyar[3,4], Nigel A. J. McMillan[3], Li Li[5], David Harrich*[1,2]

contribute equally

*corresponding author

1. Program of Infection and Inflammation, QIMR Berghofer Medical Research Institute, Herston, Queensland 4006, Australia.
2. Global Virus Network (GVN) Center of Excellence, Australian Infectious Disease Research Centre, Brisbane, QLD, Australia
3. Menzies Health Institute Queensland and School of Pharmacy and Medical Science, Griffith University, Gold Coast, Australia
4. Prorenata Biotech, Molendinar, Queensland, Australia
5. Australian Institute for Bioengineering and Nanotechnology, the University of Queensland, St Lucia, Queensland 4072, Australia

Short Title: A therapeutic RNA for dengue virus infection

Keywords: defective, interfering, RNA, DIPs, LNPs, dengue, therapeutic, antiviral, mouse

Abstract

Presently, no approved antiviral drug targets dengue virus (DENV) infection. Treatment mainly relies on supportive measures, while the efficacy of DENV vaccines varies based on factors like vaccine type, circulating DENV serotypes, and the vaccinated population. This study explores using defective interfering particles (DIPs) and lipid nanoparticles (LNPs) to deliver an anti-DENV defective interfering (DI) RNA, known as DI290. Our results showed that both DIPs and DI290 loaded LNPs (LNP-290) effectively suppressed DENV infection in human primary monocyte-derived macrophages (MDMs), THP-1 macrophages and human fibroblasts, representing cell types naturally targeted by DENV. Furthermore, LNP-290 demonstrated inhibition of DENV infection in IFNAR-deficient mice, which lack functional type I interferon (IFN) receptors, leading to decreased viremia and viral replication levels. We then proceeded to examine the involvement of IFN regulatory factor (IRF) 3 and IRF7 in facilitating DI290 RNA-triggered antiviral reactions via retinoic acid-inducible gene I (RIG-I)-like receptors (RLRs) using IRF3/IRF7 DKO mice, double knockout for IRF3 and IRF7. LNP-DI290 completely inhibited DENV infection in these DKO mice, indicating that DI290 RNA induced an IFN-mediated cellular antiviral state by a noncanonical pathway. Examination of RNA-Seq data from LNP-treated C57BL/6J mice and IFNAR-deficient mice, along with human MDMs treated with LNPs or DENV DIPs, showed that DI290 RNA treatment notably heightened IFN responses, particularly IFNγ, as well as IFNα/β and IFNλ. Furthermore, administering LNP-290 to mice did not manifest apparent adverse effects on their welfare. In summary, these experiments suggest that DI290 RNA shows potential as a therapeutic approach for combating DENV infection.

Introduction

DENV is a single-stranded RNA virus from the *Flaviviridae* family transmitted to humans by the *Aedes aegypti* mosquito. It is estimated that approximately 390 million people are infected with dengue virus each year, making it one of the most common mosquito-borne viral diseases worldwide [1]. The disease can manifest with a wide range of symptoms, from mild flu-like illness to severe and potentially fatal forms such as dengue hemorrhagic fever (DHF) and dengue shock syndrome (DSS). The development of antiviral drugs for dengue virus is crucial as they can help reduce the severity of the infection and prevent complications. Traditional antiviral drugs typically function by directly targeting the virus, either by impeding its replication or by obstructing its entry into and infection of host cells. Nonetheless, because of the absence of approved specific antiviral treatments and restricted availability of vaccines for dengue virus [2, 3], virus management primarily hinges on mosquito control measures, prompt detection and treatment of cases, and prevention of complications like fever, dehydration, bleeding and shock.

We described DI290 RNA, a short 290-nucleotide DI RNA derived from DENV [4-7]. DI RNAs are produced by RNA viruses due to errors in the viral RNA replication process. These errors lead to incomplete or shortened copies of the viral genome, which lack some or all of the genes necessary for viral replication [reviewed in 8, 9]. DI290 RNA retains the intact 5’ and 3’ untranslated regions (UTRs) of the viral genome, but it lacks all open reading frames. DI RNAs, including DI290 RNA, can disrupt the replication of the parent virus through various mechanisms. [8, 10]. Firstly, DI RNAs are suggested to compete with the parent virus for limited resources within the host cell, such as enzymes and nucleotides essential for viral replication. Secondly, DI RNAs may hinder the replication of the parent virus by acting as a

template for RNA synthesis. The viral polymerase replicates DI RNAs, producing more DI RNAs rather than viral genomic RNA. Previously, we demonstrated that DI290 RNA replicated in cells infected with DENV or Vero E6 cells expressing the DENV RNA polymerase [5]. Thirdly, DI RNAs might hinder the assembly and release of viral particles. They can compete with the viral genome for packaging signals crucial for viral assembly, leading to the production of defective viral particles, known as DIPs, which cannot infect new cells. In summary, DI RNAs contribute to controlling virus replication by restricting available resources, competing for RNA synthesis and disrupting viral assembly and release. Through these mechanisms, DI RNAs diminish the virus's capacity to propagate and induce disease.

We employed stable cell lines to synthetically generate DENV-based DIPs, which were purified and concentrated [6]. Our findings demonstrated that DIPs exhibit broad-spectrum antiviral activity by eliciting innate immune responses in cells [6]. There is evidence suggesting that DI RNAs can bind the RLRs, RIG-I and melanoma differentiation-associated protein 5 (MDA5), activating this signaling pathway and initiating antiviral responses in host cells [11, 12]. A direct interaction between the DENV 5’ UTR and RIG-I has been reported [13]. Upon recognition of a target RNA, RLRs undergo a conformational change, exposing its caspase activation and recruitment domains (CARDs). These exposed CARDs of RLRs then interact with the mitochondrial antiviral signaling protein (MAVS) located on the outer mitochondrial membrane. This interaction initiates a signaling cascade involving the activation of various downstream molecules, including TBK1 (TANK-binding kinase 1) and IKKε (I-kappa-B kinase epsilon). MAVS deficiency in cells abrogates the ability of DI RNA to induce antiviral responses to DI RNAs [14]. TBK1 and IKKε subsequently phosphorylate IRF3, IRF7 and NF-κB (Nuclear Factor-kappa B),

respectively. Phosphorylated IRF3, IRF7 and NF-κB translocate to the nucleus and induce the transcription of type I/III IFNs and other proinflammatory cytokines [reviewed in 15]. In general, DI RNAs originating from various RNA viruses have been observed to activate innate immunity and prompt an antiviral response in host cells [14, 16-19]. This event aids in regulating viral replication and dissemination.

In this study, we explored DI290's capacity to impede DENV replication in primary human macrophages, foreskin-derived fibroblasts and in two mouse models of DENV-2 infection. Our findings indicate that DI290 shows promise as an anti-DENV agent by activating IFN responses, capable of diminishing virus replication and decreasing viral titers *in vivo*. Consequently, it holds potential as a therapeutic intervention against DENV infection.

Results

DI290 RNA protects human macrophage and fibroblasts from dengue virus infection

Transmission of DENV by mosquitoes through skin bites involves several dermal and epidermal cells that are susceptible to infection, including keratinocytes, dendritic cells, Langerhans cells, and fibroblast cells [20-22]. After entering the bloodstream, DENV predominantly infects monocytes and macrophages, acting as a cellular reservoir for virus replication. [23-27]. In this study, our first objective was to examine whether DENV DIPs induce interferon responses in human primary MDMs, similar to observations made previously in Huh7 hepatoma cells [6]. MDMs treated with DENV DIPs exhibited a transient and rapid increase in IFN-β mRNA levels at 2 hours post-treatment, alongside transiently elevated levels of IFN-λ mRNA at 24

hours (Fig. 1A-B, respectively). Moreover, both RIG-I and interferon-stimulated gene 15 (ISG15) showed significant upregulation at 2 hours post-treatment and at subsequent time points (Fig. 1C-D, respectively). Similar observations were made in THP-1 macrophage cells treated with DIPs, demonstrating notable upregulation of RIG-I and ISG15 (Supplementary Fig. 1A-B). Additionally, HFF-1 cells, a human fibroblast cell lines, exhibited approximately a 2-fold increase in IFN-β mRNA levels and a 20- to 40-fold increase in RIG-I and ISG15 mRNA levels, respectively, at 24 hours post-DIP treatment (Fig. 2A-D).

Subsequently, all three cell types were infected with DENV-2 for 3 hours, employing a MOI of 0.1 for HFF-1 cells and a MOI of 1.0 for MDMs and THP-1. After removing the DENV inoculum, the cells were treated with DENV DIPs, delivering 1000 molecules of DI290 RNA per cell or with DIP storage buffer as a negative control. The viral titers in the supernatant from control-treated cells were approximately 10^3 $CCID_{50}$/mL. However, viral titers in DENV DIP-treated MDM, THP-1 and HFF-1 cells were either at the limit of detection or below (Fig. 1E, 2D and Supplementary Fig. 1C), indicating that DENV DIPs effectively inhibit DENV-2 replication *in vitro* in macrophages and fibroblasts, consistent with previous observations in other cell types [5, 6]. In summary, these findings demonstrate that DENV DIPs stimulate cellular innate immune responses with potent antiviral activity in human MDM, THP-1 and fibroblast cells.

LNPs delivering DI290 RNA inhibit DENV-2 *in vitro* and *in vivo*.

LNPs delivering DI290 RNA were used to treat MDM and HFF-1 cells *in vitro* to validate the stimulation of interferon responses [28], as observed with DIP treatment. MDMs and HFF-1 cells were treated with LNP-DI290 delivering 250 ng of DI290 for

24 hours. RT-qPCR analysis for RNA from treated and untreated cells showed that LNP-DI290 significantly upregulated IFN-β, IFN-λ, RIG-I and ISG15 mRNA levels in MDMs and HFF-1 cells compared to cells treated with empty LNPs and untreated cells after 24 hours (Fig. 3A-D and 4A-C). These results demonstrate that LNPs effectively deliver DI290 RNA, stimulating innate immune responses and upregulating IFNs and ISGs in MDMs and HFF-1 cells.

Subsequently, MDMs and HFF-1 cells were infected with DENV-2 and treated with LNP-290 as in previous experiments. As depicted in figures 3E and 4D, cells treated with LNP-290 exhibited strong inhibition of DENV-2 compared to cells treated with empty LNPs and untreated cells.

LNPs have the capability to deliver significant amounts of RNA *in vivo*, which prompted us to evaluate the antiviral efficacy of LNP-DI290 in a DENV-mouse model. IFNAR-deficient mice are genetically modified to have a specific deletion of the gene encoding the interferon-alpha/beta receptor 1 (IFNAR-deficient). This receptor is a critical component of the signaling pathway for type I interferons. By knocking out the *Ifnar1* gene, these mice lack the receptor necessary for cells to respond to type I interferons, thereby exhibiting heightened susceptibility to infections by viruses, including DENV [29]. IFNAR-deficient mice were infected by intraperitoneal (*i.p.*) injection of mouse-adapted D220 DENV-2 strain (10^4 $CCID_{50}$ per mouse), followed by treatment with LNP-290 delivering 15 µg of RNA, empty LNPs or buffer only at 4 hours post-infection (h.p.i) (Fig. 5A). Serum and spleen samples were collected at 72 h.p.i. and subjected to assays for infectious virus or viral RNA. Infectious D220 was detected in the spleen at >3 Log_{10} $CCID_{50}$/mL, while infectious virus was undetectable in the spleen and serum samples from mice treated with LNP-290 (Fig. 5B-C). Conversely, all samples from untreated and empty LNP-

treated mice exhibited measurable titers of D220, indicating the antiviral activity of LNP-DI290 *in vivo*.

RT-qPCR analysis of total RNA isolated from splenic samples of all mice showed a significant decrease in viral RNA in LNP-290 treated mice compared to mice treated with empty LNPs or buffer (Fig. 5D). This indicates that mice treated with LNP-DI290 were infected by DENV-2 but did not result in measurable levels of viremia *in vivo*. Finally, LNP-290 treated mice did not observe significant weight loss, suggesting that DENV infection and LNP-DI290 treatment did not induce an acute metabolic or other adverse change over the course of the experiment. The combined data show that LNP-DI290 delivering 15 µg of DI290 RNA strongly inhibited D220 replication and reduced viremia in IFNAR-deficient mice without apparent adverse effects.

LNP-DI290 can protect mice from DENV infection independent of IRF3/7.

DENV infection leads to the activation of innate immune responses involving several pattern recognition receptors (PRRs) including Toll-like receptor (TRL) 3 [30], TLR7 [31] and the RLRs RIG-I and MDA5 [32], among others. IRF3 and IRF7, the two family members with the greatest structural homology, are principal mediators of type I IFN induction [reviewed in 33]. We used IRF3/IRF7 DKO infected with D220 and then treated them with LNP-DI290, empty LNP or buffer (Fig. 6A). Viremia in serum at >2.5 Log_{10} $CCID_{50}$/mL and viral titre in spleen tissue at >3 Log_{10} $CCID_{50}$/mL was detected after 3 d.p.i (Fig. 6B-C). However, in LNP-DI290 treated mice, no virus was detected in serum or spleen samples. We measured viral RNA in total spleen RNA samples from all mice (Fig. 6D), but no viral RNA was detected in mice treated with LNP-DI290 (Fig. 6D). As observed for IFNAR-deficient mice, significant weight loss was not observed over the course of the experiment in these mice (Fig. 6E).

Given the importance of RIG-I and MDA5 in establishing innate immune responses to DENV infection [32], this outcome indicates, surprisingly, that DI290 RNA induced innate immune responses in mice that strongly inhibited DENV in an IRF3/7 independent manner.

Activation of innate immune response including IFN-γ following treatment of DENV DIPs and LNP-DI290 *in vivo* and *in vitro.*

Activation of the innate immune response following treatment with DENV DIPs and LNP-DI290 was examined both *in vivo* and *in vitro*. To investigate host responses after treatment with DENV DIPs/LNP-DI290, we employed RNA sequencing (RNA-Seq) to quantitatively measure the expression levels of transcripts in spleen tissues from both C57BL/6J and IFNAR-deficient mice treated with LNP-DI290 or empty LNPs. Additionally, we analyzed RNA from MDMs treated with LNP-DI290 and empty LNPs. We also included DENV DIP-treated MDMs to compare induction patterns following LNP treatment versus DIP treatment.

Approximately 10% of genes in the human genome have the potential to be regulated by IFNs [34]. The RNA-Seq analysis revealed substantial transcriptional alterations in host cells induced by DENV DIP/LNP-DI290 treatment (Supp. #. RNA Seq raw data). A total of 87 upregulated genes were commonly identified in mouse spleen tissues and human MDMs (Fig. 7). Notably, over 45 shared upregulated genes in response to these treatments represented interferon-stimulated genes (ISGs), including ZPB1, MX1, ISG15, IFIT1-3, IFITM3, and OAS2-3, among others. IFNs, as secreted cytokines, activate signal transduction cascades leading to the induction of hundreds of ISGs. ISGs upregulated in MDMs and mice in this study, which were previously reported to inhibit DENV replication, include ISG15 [35], 2′,5′-

oligoadenylate synthetase (OAS) 3 [36], IFITM3 [37], BST2 (Viperin) [37, 38] , and CMPK2 [39]. In addition, PRRs, including RIG-I, MDA5 (IFIH1) and LGP2, were upregulated by DI290 RNA even in IFNAR-deficient mice where IFNα/β is impeded.

To explore the cellular responses further, the outcomes of RNA-Seq analysis were subjected to canonical pathway analysis (CPA) CORE analysis to identify common upregulated or downregulated upstream regulatory sequences (USRs) after DIP or LNP-290 treatment. In figure 8, the heatmaps show activation Z-scores of cytokine/chemokine USRs (Fig. 8A) and transcriptional regulators USRs (Fig 8B) that were significantly upregulated. The analysis showed activation of 117 cytokines/chemokines that include IFN-γ (IFNG), TNF, IFN-α (IFNA1 and IFNA2), IFN-β (IFNB1) and IFN-λ (IFNL1). The activation Z-score of IL-27 is consistent with the regulation of both innate and adaptive immunity USRs [40]. IL-27 can induce IFN-γ and inflammatory mediators from T lymphocytes and innate immune cells [41]. The activation Z-scores of IRFs included IRF1, IRF3, IRF5, IRF7 and IRF9 (Fig 8B). Other activation Z-scores for transcription factors include Zbtb10, which is involved in dendritic cell activation [42], STAT1, STAT2, and NFκB (NFKB1, NFKB2), which regulate inflammatory responses. Taken together, the observed modulation of key inflammatory regulators, particularly the activation of IFNs and associated immune effectors, demonstrates that DENV DIP/LNP-DI290 treatment triggers a robust innate immune response when stimulated by DI290 RNA *in vitro* and *in vivo*.

Discussion

Here, we showed that DI290 RNA, a naturally derived DENV-2 DI RNA [4], triggers host cell antiviral responses, effectively suppressing DENV infection both *in vitro* and

in vivo. DI RNA belongs to the class of defective viral genomes (DVGs), which emerge during viral replication within cells and are packaged and released as non-infectious virus-like particles (VLPs) alongside infectious wild-type viruses. [10, 43]. The presence of these VLPs in a virus stock is linked with reduced viral replication and virulence, indicating attenuation [14, 44-46]. In this study, we utilized DI290 RNA delivered through DIPs or LNPs to activate cellular innate immune responses capable of counteracting DENV replication. DENV employs well-characterized mechanisms to evade the innate antiviral response. For instance, DENV NS3 can inhibit RIG-I activation [47], while the DENV NS5 protein disrupts IFN signaling by binding to and degrading STAT2 [48-50]. For Sendai virus, DVGs possess the capability to overcome virus-mediated inhibition of IFN induction, potentially through preferential binding of a DVG to RIG-I or MDA5 compared to the wild-type genome [14]. It is plausible that DI290 may exhibit preferential binding to an RLR such as RIG-I, thereby inducing IFN responses in DENV-infected cells. This possibility could be further investigated in future studies, for instance, utilizing techniques like RNAscope [51].

The IPA analysis of RNAseq data revealed that DI RNA notably upregulated IFN-γ signaling in MDM cells, IFNAR-deficient mice and C57BL/6J mice. IFNAR-deficient mice are susceptible to DENV infection due to impaired IFN-α/β signaling and diminished antiviral responses. However, treatment with LNP-DI290 significantly reduced viremia and virus replication in splenic tissue. Our analysis suggests that IFN-γ signaling may have facilitated the upregulation of ISGs, inhibiting DENV replication in IFNAR mice. Notably, IFN-γ signaling is protective against DENV pathogenesis in vaccinated individuals [52] and in IFNAR mice [53]. RNA-Seq Z-scores indicated a significant increase in TNF, IFN-γ, and IFN-λ1. This finding

supports the notion that DI290 RNA exerts its effect in IFNAR-deficient mice by upregulating antiviral activity. Further support for this possibility was observed in experiments using IRF3/IRF7 DKO mice. In all systems treated with LNP-DI290 or DIPs, similar patterns of pathway activation in DEGs, cytokine/chemokine and transcriptional regulators were evident. The PRRs that trigger antiviral responses upon infection, including TLR3, TLR7, RIG-I and MDA5, induce both type I and type III IFNs via IRF3 and IRF7. Notably, viral infection was not detected in IRF3/IRF7 DKO mice treated with LNP-290, which lack IFN type I expression but retain functional IFN type I receptors. DI290 RNA may stimulate noncanonical IFN activation pathways in MDMs, IFNAR mice and IRF3/IRF7 DKO mice, resulting in the upregulation of IFN-driven antiviral responses.

Activation of signaling pathways by DI RNA may lead to unintended consequences, including off-target effects that could be harmful. Excessive activation of the immune system, particularly if sustained, can result in immunotoxicity. We conducted preliminary testing of LNP-DI290 in IFNAR-deficient and C57BL/6J mice, where the delivery of DI290 RNA in IFNAR-deficient and IRF3/IRF7 DKO mice did not cause any significant levels of weight loss, an indicator no serious metabolic change. It is possible that the efficacy and safety of DI290 may depend on the dose, and finding the right balance between stimulating the immune response and avoiding adverse effects will be crucial.

This study showed that LNP-DI290 administered to infected mice 4 h.p.i. prevented viremia in infected. Treatment timing in this model was limited due to rapid peak viremia (at 3 d.p.i.) and viral clearance (at 4-5 d.p.i) in *Ifnar*$^{-/-}$ mice. Future studies to investigate if prophylactic LNP-DI290 application is protective, or if administration at a later time point post-infection provides protection from infection, is warranted but a

different approach and animal model may be necessary. For example, AG129 mice, which have KO for both type I and type II IFN receptors, permit higher levels of viral replication compared to IFNAR mice. A recent study showed that both models resulted in a similar time course with respect to viremia. Interestingly, aspects of severe dengue disease were recapitulated by both models involving DENV-mediated inflammation and tissue damage in the gastrointestinal tract (GIT) [54]. The GIT pathology occurred late in the disease after the peak of viremia. Infected macrophage but not endothelial cells in the GIT were reported. Whether DI290 RNA therapy ameliorates or exacerbates GIT pathology could help define the utility of DI290 therapy during the late stages of DENV disease.

In summary, we have demonstrated that DI290 RNA delivered by DIPs or LNP-290 activates innate immune responses in macrophages, a primary target for DENV infection, and strongly inhibits DENV infection in THP-1 and human MDMs. LNP-DI290 strongly inhibited DENV replication in IFNAR-deficient mice and IRF3/IRF7 DKO mice. Control of DENV replication was associated with solid upregulation of IFN signaling pathways. Under the conditions tested, a single dose post-infection treatment did not appear to cause adverse events in these animal models, indicating that DI290 RNA has potential as a therapy for DENV infection.

Methods and Materials

Ethics statement

All mouse work was conducted in accordance with the “Australian code for the care and use of animals for scientific purposes” as defined by the National Health and Medical Research Council of Australia. All animal procedures were performed in accordance with protocols approved by the QIMR Berghofer Medical Research

Institute Animal Ethics Committee (P2277, A2002-600). Mice were euthanized using carbon dioxide asphyxiation.

Cell culture

Vero E6 and HFF-1 cells were maintained in Dulbecco's Modified Eagle medium (DMEM) (Thermo Fisher) supplemented with 10% (v/v) fetal bovine serum (FBS) (Thermo Fisher) and 1% (v/v) penicillin-streptomycin (Thermo Fisher). DENV DIP-producing cell line, HEK-DI-290-ORF, was cultured in HEK GM Serum-Free Medium (Sartorius) supplemented with 1% (v/v) penicillin-streptomycin, 1% (v/v) GlutaMAX-I (Thermo Fisher) and 50 nM PEP005 during DENV DIP production. The human monocytic cell line THP-1 was maintained in Roswell Park Memorial Institute (RPMI) 1640 medium supplemented with 10% (v/v) FBS and 1% (v/v) penicillin-streptomycin. For experiments, THP-1 cells were differentiated into macrophage-like cells by stimulation of 50 ng/mL phorbol myristate acetate (PMA) for 48 h. The THP-1 cells were thereafter rested for 24 h by replacing the PMA-containing medium with a complete medium. All cells were incubated at 37 °C in a humidified 5% CO_2 atmosphere. C6/36 cells were grown in DMEM supplemented with 10% (v/v) FBS and 1% (v/v) penicillin-streptomycin

Isolation of monocytes from peripheral blood mononuclear cells (PBMC)

PBMCs were isolated from a healthy donor's buffy coat supplied by the Australian Red Cross Blood Service using Ficoll density gradient centrifugation as previously described [55]. After PBMC isolation, cells were washed and resuspended in PBS containing 2% FBS and 1 mM EDTA. Monocytes were isolated from PBMCs using EasySep™ Human CD14 Positive Selection Kit according to the manufacturer's instructions (Stemcell Technologies).

Differentiation of monocyte to MDMs

MDMs were differentiated as previously described [56]. Briefly, Isolated monocytes were cultured in RPMI 1640 (Thermo Fisher) supplemented with 10% (v/v) FBS, 1% (v/v) penicillin-streptomycin, 10 ng/mL macrophage colony-stimulating factor (M-CSF) (Thermo Fisher) and 1 ng/mL granulocyte-macrophage colony-stimulating factor (GM-CSF) (Thermo Fisher) for 5 days. Media were changed every 2 days.

LNP-20 Formulation.

LNPs encapsulating DI290 RNA, were created using the hydration method [57]. Briefly, required amounts of lipid and PEG2000- C16Ceramide were mixed with DI290 RNA at an N:P ratio of 4 in a sucrose-containing water/tert-butanol (1:1 v/v) co-solvent system. DOTAP, cholesterol, DOPE and PEG2000-C16Ceramide with a molar ratio of 50:35:5:10 was used. The mixture was then snap-frozen and freeze-dried overnight. Freeze-dried matrix was then hydrated with sterile water immediately before use at a concentration of 0.1mg/ml D1290 final.

Analysis of DENV DIP and LNP-DI290 antiviral activity in vitro

HFF-1, MDM and THP-1 were seeded in 48-well plates with 10,000 cells per well. THP-1 cells were induced for differentiation, as described above. The next day, the cells were infected with DENV-2 (MOI=0.1 $CCID_{50}$ per cell for THP-1 and MOI=1 $CCID_{50}$ per cell for THP-1 and MDM). After 3 h, the cells were washed with 1X PBS and incubated with either culture medium alone, medium containing DENV DIP (at a dosage equivalent to 1,000 DI290 RNA copies (=0.2 fg) per cell), empty LNP or LNP-DI290 (at a dosage equivalent to 1.6 X 10^8 DI290 RNA copies (=25 pg) per cell). At 3 days post-infection, the viral titers were determined by $CCID_{50}$ assays as previously described [6, 58].

Gene expression analysis

HFF-1, MDM and THP-1 cells were seeded at a density of 50,000 each well in a 48-well plate. THP-1 cells were induced for differentiation, as described above. The next day, the cells were treated with culture medium only or medium containing either DENV DIP (equivalent to 1,000 DI290 RNA copies (= 0.2 fg) / cell), empty LNP or LNP-DI290 (equivalent to 1.6 X 108 DI290 RNA copies (= 25 pg) / cell). Total RNA from cells was extracted after 2 h, 24 h, 48 h and 72 h treatment using RNeasy Kit (Qiagen) and mRNA expression levels of Ribosomal Protein L13a (RPL13A), IFN-β, RIG-I and ISG15 were determined using Luna Universal One-Step RT-qPCR Kit according to the manufacturer's instructions (New England Biolabs). The primer sequences are available upon request. The data was normalized to RPL13A as the reference gene and presented as fold change relative to untreated control cells using $\Delta\Delta C_t$ method.

DENV DIP production, precipitation and chromatographic purification

HEK-DI-290-ORF cells were seeded at 2.5 x 10^5 cells/ml and grown in a ProCulture glass spinner flask (Corning) using a magnetic stir plate (Thermo Fisher) set at 65 rpm. After 48 h, the culture supernatant containing DENV DIPs was collected, filtered through a 0.22 µm filter (Merck Millipore), and the clarified supernatant was stored at 4 °C. The clarified supernatant was processed through the tangential flow filtration (TFF) system (AKTA Flux S, Cytiva), which was equipped with 100 kDa molecular weight cut-off filter (UFP-100-C-H24LA hollow fiber cartridge) and equilibrated with sterile 1X PBS. Upon equilibration, the clarified supernatant was added to the TFF chamber and flowed through 54 mL/min and a permeate pump rate of 5 mL/min. The transmembrane pressure was maintained below 0.5 bar. The resulting concentrated

retentate was then filtered through a 0.22 µm filter and added with stabilizing buffer containing 2% (v/v) glycerol and 5% (v/v) sorbitol before CHT ceramic hydroxyapatite chromatographic purification of DENV DIPs.

CHT chromatography column purification was performed as previously described [6]. The resulting purified DENV DIPs were then concentrated using an Amicon Ultra-15 centrifugal filter unit (50 kDa cutoff) until the volume was reduced to around 1-1.5 mL. Quantification of DI290 RNA copies was performed by qPCR analysis.

Mouse infection

All mice were bred in-house and housed at QIMR Berghofer Medical Research Institute, Brisbane, QLD, Australia. IFNAR-deficient mice [59] and IRF3/IRF7 DKO mice [60] were infected *i.p.* with 1 x 10^4 $CCID_{50}$ of DENV-2 strain D220 for 4 h. Mock-infected mice were injected i.p. with PBS. After 4 h infection, the mice were treated i.p. with either LNP-DI290 containing 15 µg of DI290 RNA or empty LNPs. Following treatment, body weight and general conditions were monitored daily for up to 3 days. The mice were euthanized using CO_2 at 3 days post infection. Blood was harvested through heart puncture and the spleen was collected and homogenized in 1 ml RPMI 1640 containing 2% FBS. A 200 µl of the homogenate was mixed with Trizol (Thermo Fisher) for RNA extraction, followed by quantification of viral RNA using RT-qPCR. Virus titration in both blood and spleen samples was determined by $CCID_{50}$ assays as previously described [6, 58].

Quantification of viral RNA from spleen samples

After Trizol extraction, the RNA pellet was resuspended in 50 µl of RNase-free H_2O and 1 µl of the resuspended samples was used for quantification of the DENV-2 D220 NS5 RNA regions using Luna Universal One-Step RT-qPCR Kit (New England

Biolabs) in a 10-ul reaction volume. The thermal cycling conditions were as follows: 15 min at 55 °C, 2min at 95 °C and 40 cycles of 5 sec at 95 °C, 45 sec at 55 °C (data acquisition) and 15 sec at 72 °C. The primer sequences are available on request.

mRNA seq sample library preparation and analysis

For the preparation of MDM mRNA, MDMs were seed in 48-well plates with 30,000 cells per well and treated with either culture medium alone, medium containing DENV DIP (at a dosage equivalent to 0.2 fg DI290 RNA copies per cell, n=3), empty LNP (n=3) or LNP-DI290 (at a dosage equivalent to 25 pg DI290 RNA copies per cell, n=3). After 24 treatments, total RNA was extracted from the cells using RNeasy Kit (Qiagen) according to the manufacturer's instructions. For mRNA preparation from mouse spleens, C57BL/6J (n=6) and IFNAR-deficient (n=5) mice were *i.p.* treated with empty LNP or LNP-DI290 (at a dosage equivalent to 15 μg DI290 RNA per mouse). After 24 hours of treatment, whole spleens were harvested, preserved in RNA*later*™ solution (Thermo Fisher) and homogenized in Trizol (Thermo Fisher). Total spleen RNA was then extracted following the manufacturer's instructions.

RNA concentration and quality were measured using TapeStation D1kTapeScreen assay (Agilent). cDNA libraries were generated using Illumina TruSeq Stranded mRNA library prep kit and were sequenced using an Illumina Nextseq 2000 Sequencing System to produce 75nt paired-end reads. Sequence reads were aligned to either the GRCm39 v33 mouse or the GRCh38 v44 human reference genomes obtained from Gencode, using STAR aligner v2.7.10. Aligned read counts were calculated for each annotated gene using RSEM v1.3.1, and differential expression was estimated with EdgeR v3.42.4 using the statistical software, R v4.2.0. Only genes with at least 0.5 counts-per-million (approximately 10 aligned

reads) were included in the test for differential expression. Significantly differentially expressed genes (DEGs) were analyzed using Ingenuity Pathway Analysis v107193442 (QIAGEN). IPA accepts DEG sets of between 200-3000 genes. Therefore, false discovery rate (FDR) cut-offs were adjusted to keep DEG sets within this range and roughly comparable between experimental groups. q<1x10-2 was used for the C57BL/6J group; q<1x10-5 was used for the IFNAR-deficient group; q<1x10-3 was used for the DIP-treated MDM group; q<1x10-5 was used for the LNP-DI290-treated MDM group.

Statistical analysis

Statistical analysis was performed using IMB SPSS Statistics (IMB Corp.) and GraphPad Prism (GraphPad software). The *t*-test was used when the difference in variances was <4, skerness was >-2, and Kurtosis was <2. Otherwise, the nonparametric Kolmogorov-Smirnov test was used. *p*-value <0.05 was considered significant.

Acknowledgements

This research was generously supported through funding from the Wellcome Trust Innovator Award 219588Z/19/Z to D.H. and the DARPA INTERfering and Co-Evolving Prevention and Therapy (INTERCEPT) program to D.H. and John Aaskov. We sincerely thank John Aaskov for the introduction to dengue virus defective interfering particles field. We also thank Dr. I Anraku for his assistance in managing the PC3 (BSL3) facility at QIMR Berghofer Medical Research Institute and animal house staff from QIMR Berghofer Medical Research Institute for mouse breeding and agistment.

References

1. *World Health Organization Disease Outbreak News; Dengue – Global situation*. 2023; Available from: https://www.who.int/emergencies/disease-outbreak-news/item/2023-DON498
2. Deng, S.Q., et al., *A Review on Dengue Vaccine Development.* Vaccines (Basel), 2020. **8**(1).
3. Palanichamy Kala, M., A.L. St John, and A.P.S. Rathore, *Dengue: Update on Clinically Relevant Therapeutic Strategies and Vaccines.* Curr Treat Options Infect Dis, 2023. **15**(2): p. 27-52.
4. Li, D. and J. Aaskov, *Sub-genomic RNA of defective interfering (D.I.) dengue viral particles is replicated in the same manner as full length genomes.* Virology, 2014. **468-470**: p. 248-255.
5. Li, D., et al., *Dengue virus-free defective interfering particles have potent and broad anti-dengue virus activity.* Commun Biol, 2021. **4**(1): p. 557.
6. Lin, M.H., et al., *Defective Interfering Particles with Broad-Acting Antiviral Activity for Dengue, Zika, Yellow Fever, Respiratory Syncytial and SARS-CoV-2 Virus Infection.* Microbiol Spectr, 2022. **10**(6): p. e0394922.
7. Li, D., et al., *Defective interfering viral particles in acute dengue infections.* PLoS One, 2011. **6**(4): p. e19447.
8. Vignuzzi, M. and C.B. Lopez, *Defective viral genomes are key drivers of the virus-host interaction.* Nat Microbiol, 2019. **4**(7): p. 1075-1087.
9. Genoyer, E. and C.B. Lopez, *The Impact of Defective Viruses on Infection and Immunity.* Annu Rev Virol, 2019. **6**(1): p. 547-566.
10. Huang, A.S. and D. Baltimore, *Defective viral particles and viral disease processes.* Nature, 1970. **226**(5243): p. 325-7.
11. Baum, A., R. Sachidanandam, and A. Garcia-Sastre, *Preference of RIG-I for short viral RNA molecules in infected cells revealed by next-generation sequencing.* Proc Natl Acad Sci U S A, 2010. **107**(37): p. 16303-8.
12. Linder, A., et al., *Defective Interfering Genomes and the Full-Length Viral Genome Trigger RIG-I After Infection With Vesicular Stomatitis Virus in a Replication Dependent Manner.* Front Immunol, 2021. **12**: p. 595390.
13. Chazal, M., et al., *RIG-I Recognizes the 5' Region of Dengue and Zika Virus Genomes.* Cell Rep, 2018. **24**(2): p. 320-328.
14. Tapia, K., et al., *Defective viral genomes arising in vivo provide critical danger signals for the triggering of lung antiviral immunity.* PLoS Pathog, 2013. **9**(10): p. e1003703.
15. Rehwinkel, J. and M.U. Gack, *RIG-I-like receptors: their regulation and roles in RNA sensing.* Nature Reviews Immunology, 2020. **20**(9): p. 537-551.
16. Wang, C., et al., *Influenza Defective Interfering Virus Promotes Multiciliated Cell Differentiation and Reduces the Inflammatory Response in Mice.* J Virol, 2023. **97**(6): p. e0049323.
17. Sun, Y., et al., *Immunostimulatory Defective Viral Genomes from Respiratory Syncytial Virus Promote a Strong Innate Antiviral Response during Infection in Mice and Humans.* PLoS Pathog, 2015. **11**(9): p. e1005122.
18. Welch, S.R., et al., *Inhibition of Nipah Virus by Defective Interfering Particles.* J Infect Dis, 2020.
19. Xiao, Y., et al., *A defective viral genome strategy elicits broad protective immunity against respiratory viruses.* Cell, 2021. **184**(25): p. 6037-6051 e14.
20. Rathore, A.P.S. and A.L. St John, *Immune responses to dengue virus in the skin.* Open Biol, 2018. **8**(8).
21. Kurane, I., J. Janus, and F.A. Ennis, *Dengue virus infection of human skin fibroblasts in vitro production of IFN-beta, IL-6 and GM-CSF.* Arch Virol, 1992. **124**(1-2): p. 21-30.

22. Wei, K.C., et al., *Discrepant Activation Pattern of Inflammation and Pyroptosis Induced in Dermal Fibroblasts in Response to Dengue Virus Serotypes 1 and 2 and Nonstructural Protein 1.* Microbiol Spectr, 2023. **11**(1): p. e0358622.
23. Kou, Z., et al., *Monocytes, but not T or B cells, are the principal target cells for dengue virus (DV) infection among human peripheral blood mononuclear cells.* J Med Virol, 2008. **80**(1): p. 134-46.
24. Kyle, J.L., P.R. Beatty, and E. Harris, *Dengue virus infects macrophages and dendritic cells in a mouse model of infection.* J Infect Dis, 2007. **195**(12): p. 1808-17.
25. Halstead, S.B., E.J. O'Rourke, and A.C. Allison, *Dengue viruses and mononuclear phagocytes. II. Identity of blood and tissue leukocytes supporting in vitro infection.* J Exp Med, 1977. **146**(1): p. 218-29.
26. Zellweger, R.M., T.R. Prestwood, and S. Shresta, *Enhanced infection of liver sinusoidal endothelial cells in a mouse model of antibody-induced severe dengue disease.* Cell Host Microbe, 2010. **7**(2): p. 128-39.
27. Prestwood, T.R., et al., *Trafficking and replication patterns reveal splenic macrophages as major targets of dengue virus in mice.* J Virol, 2012. **86**(22): p. 12138-47.
28. Idris, A., et al., *A SARS-CoV-2 targeted siRNA-nanoparticle therapy for COVID-19.* Mol Ther, 2021. **29**(7): p. 2219-2226.
29. Chan, K.W., et al., *Animal models for studying dengue pathogenesis and therapy.* Antiviral Res, 2015. **123**: p. 5-14.
30. Tsai, Y.T., et al., *Human TLR3 recognizes dengue virus and modulates viral replication in vitro.* Cell Microbiol, 2009. **11**(4): p. 604-15.
31. Wang, J.P., et al., *Flavivirus activation of plasmacytoid dendritic cells delineates key elements of TLR7 signaling beyond endosomal recognition.* J Immunol, 2006. **177**(10): p. 7114-21.
32. Loo, Y.M., et al., *Distinct RIG-I and MDA5 signaling by RNA viruses in innate immunity.* J Virol, 2008. **82**(1): p. 335-45.
33. Jefferies, C.A., *Regulating IRFs in IFN Driven Disease.* Front Immunol, 2019. **10**: p. 325.
34. Schoggins, J.W., *Interferon-Stimulated Genes: What Do They All Do?* Annu Rev Virol, 2019. **6**(1): p. 567-584.
35. Dai, J., W. Pan, and P. Wang, *ISG15 facilitates cellular antiviral response to dengue and west nile virus infection in vitro.* Virol J, 2011. **8**: p. 468.
36. Lin, R.J., et al., *Distinct antiviral roles for human 2',5'-oligoadenylate synthetase family members against dengue virus infection.* J Immunol, 2009. **183**(12): p. 8035-43.
37. Jiang, D., et al., *Identification of five interferon-induced cellular proteins that inhibit west nile virus and dengue virus infections.* J Virol, 2010. **84**(16): p. 8332-41.
38. Pan, X.B., et al., *BST2/tetherin inhibits dengue virus release from human hepatoma cells.* PLoS One, 2012. **7**(12): p. e51033.
39. Pawlak, J.B., et al., *CMPK2 restricts Zika virus replication by inhibiting viral translation.* PLoS Pathog, 2023. **19**(4): p. e1011286.
40. Trinchieri, G., S. Pflanz, and R.A. Kastelein, *The IL-12 family of heterodimeric cytokines: new players in the regulation of T cell responses.* Immunity, 2003. **19**(5): p. 641-4.
41. Trinchieri, G., *Interleukin-12 and the regulation of innate resistance and adaptive immunity.* Nat Rev Immunol, 2003. **3**(2): p. 133-46.
42. Smita, S., et al., *Zbtb10 transcription factor is crucial for murine cDC1 activation and cytokine secretion.* Eur J Immunol, 2021. **51**(5): p. 1126-1142.
43. Von Magnus, P., *Incomplete forms of influenza virus.* Adv Virus Res, 1954. **2**: p. 59-79.
44. Barrett, A.D. and N.J. Dimmock, *Modulation of a systemic Semliki Forest virus infection in mice by defective interfering virus.* J Gen Virol, 1984. **65 (Pt 10)**: p. 1827-31.

45. Rabinowitz, S.G. and J. Huprikar, *The influence of defective-interfering particles of the PR-8 strain of influenza A virus on the pathogenesis of pulmonary infection in mice.* J Infect Dis, 1979. **140**(3): p. 305-15.
46. Scott, P.D., et al., *Defective interfering virus protects elderly mice from influenza.* Virol J, 2011. **8**: p. 212.
47. Chan, Y.K. and M.U. Gack, *A phosphomimetic-based mechanism of dengue virus to antagonize innate immunity.* Nat Immunol, 2016. **17**(5): p. 523-30.
48. Ashour, J., et al., *NS5 of dengue virus mediates STAT2 binding and degradation.* J Virol, 2009. **83**(11): p. 5408-18.
49. Mazzon, M., et al., *Dengue virus NS5 inhibits interferon-alpha signaling by blocking signal transducer and activator of transcription 2 phosphorylation.* J Infect Dis, 2009. **200**(8): p. 1261-70.
50. Morrison, J., et al., *Dengue virus co-opts UBR4 to degrade STAT2 and antagonize type I interferon signaling.* PLoS Pathog, 2013. **9**(3): p. e1003265.
51. Ball, J.B., et al., *Combining RNAscope and immunohistochemistry to visualize inflammatory gene products in neurons and microglia.* Front Mol Neurosci, 2023. **16**: p. 1225847.
52. Gunther, V.J., et al., *A human challenge model for dengue infection reveals a possible protective role for sustained interferon gamma levels during the acute phase of illness.* Vaccine, 2011. **29**(22): p. 3895-904.
53. Prestwood, T.R., et al., *Gamma interferon (IFN-gamma) receptor restricts systemic dengue virus replication and prevents paralysis in IFN-alpha/beta receptor-deficient mice.* J Virol, 2012. **86**(23): p. 12561-70.
54. Pliego Zamora, A., et al., *Kinetics of severe dengue virus infection and development of gut pathology in mice.* J Virol, 2023. **97**(11): p. e0125123.
55. Apolloni, A., et al., *A mutant Tat protein provides strong protection from HIV-1 infection in human CD4+ T cells.* Hum Gene Ther, 2013. **24**(3): p. 270-82.
56. Nielsen, M.C., M.N. Andersen, and H.J. Moller, *Monocyte isolation techniques significantly impact the phenotype of both isolated monocytes and derived macrophages in vitro.* Immunology, 2020. **159**(1): p. 63-74.
57. Wu, S.Y., et al., *Development of a novel method for formulating stable siRNA-loaded lipid particles for in vivo use.* Pharm Res, 2009. **26**(3): p. 512-22.
58. Setoh, Y.X., et al., *De Novo Generation and Characterization of New Zika Virus Isolate Using Sequence Data from a Microcephaly Case.* mSphere, 2017. **2**(3).
59. Swann, J.B., et al., *Type I IFN contributes to NK cell homeostasis, activation, and antitumor function.* J Immunol, 2007. **178**(12): p. 7540-9.
60. Rudd, P.A., et al., *Interferon response factors 3 and 7 protect against Chikungunya virus hemorrhagic fever and shock.* J Virol, 2012. **86**(18): p. 9888-98.

Figure legends

Figure 1. DENV DIPs stimulate host innate immune responses in human primary MDMs and inhibit DENV-2 replication. (A-D) Monocytes were isolated from human PBMCs using CD14 positive selection and maturated to MDMs with M-CSF and GM-CSF for 5 days. MDMs were then treated with DENV DIPs (at a dosage equivalent to 1,000 DI290 RNA copies (=0.2 fg) per cell) for 2, 24, 48 and 72 h. Total RNA was extracted from the cells and the levels of IFN-β, IFN-λ, RIG-I and ISG15 mRNA were quantified by RT-qPCR. The fold change relative to the untreated control cells was calculated (n=3). (E) MDMs were infected with DENV-2 (MOI=1 $CCID_{50}$ per cell). After 3 h, the cells were washed with 1X PBS and incubated with culture medium containing DENV DIP (at a dosage equivalent to 1,000 DI290 RNA copies (=0.2 fg) per cell). DENV-2 titers in culture supernatant were measured by $CCID_{50}$ assay at 3 days post-infection (n=3). The data are shown as the mean ± standard of deviation (SD). P values were calculated using a two-tailed Student's *t* test. L.D.: limit of detection. ns: not significant.

Figure 2. DENV DIPs activate IFN responses and inhibits DENV-2 in HFF-1 human fibroblast cells. (A-C) HFF-1 cells were treated with DENV DIP (at a dosage equivalent to 1,000 DI290 RNA copies (=0.2 fg) per cell) for 24 h. Total RNA was extracted from the cells and the levels of IFN-β, RIG-I, and ISG15 mRNA were quantified by RT-qPCR. The fold change relative to the untreated control cells was calculated (n=3). (D) HFF-1 cells were infected with DENV-2 (MOI=0.1 $CCID_{50}$/cell). After 3 h, the cells were washed with 1X PBS and incubated with culture medium containing DENV DIP (at a dosage equivalent to 1,000 DI290 RNA copies (=0.2 fg) per cell). DENV-2 titers in culture supernatant were measured by $CCID_{50}$ assay at 3

days post-infection (n=3). Data are shown as the mean ± SD. P values were calculated using a two-tailed Student's *t* test.

Figure 3. LNP-DI290 stimulates host innate immune responses in human primary MDMs and inhibits DENV-2 replication. (A-D) MDMs were treated with LNP-DI290 (at a dosage equivalent to 25 pg DI290 RNA per cell) for 2, 24, 48 and 72 h. Total RNA was extracted from the cells and the levels of IFN-β, IFN-λ, RIG-I and ISG15 mRNA were quantified by RT-qPCR. The fold change relative to the untreated control cells was calculated (n=3). (E) MDM were infected with DENV-2 (MOI=1 $CCID_{50}$ per cell). After 3 h, the cells were washed with 1X PBS and incubated with either culture medium alone, medium containing either empty LNP or LNP-DI290 (at a dosage equivalent to 25 pg DI290 RNA per cell). DENV-2 titers in culture supernatant were measured by $CCID_{50}$ assay at 3 days post-infection (n=3). Data are shown as the mean ± SD. P values were calculated using a two-tailed Student's *t* test. L.D.: limit of detection. ns: not significant.

Figure 4. LNP-DI290 stimulates host innate immune responses in HFF-1 cells and inhibits DENV-2 replication. (A-C) HFF-1 cells were treated with empty LNP or LNP-DI290 (at a dosage equivalent to 25 pg DI290 RNA per cell) for 24 h. Total RNA was extracted from the cells and the levels of IFN-β, RIG-I and ISG15 mRNA were quantified by RT-qPCR. The fold change relative to the untreated control cells was calculated (n=3). (D) HFF-1 cells were infected with DENV-2 (MOI=0.1 $CCID_{50}$ per cell). After 3 h, the cells were washed with 1×PBS and incubated with either culture medium alone, medium containing empty LNP or LNP-DI290 (at a dosage equivalent to 25 pg DI290 RNA per cell). DENV-2 titers in culture supernatant were measured by $CCID_{50}$ assay at 3 days post-infection (n=3). Data are shown as the mean ± SD. P

values were calculated using a two-tailed Student's *t* test. L.D.: limit of detection. ns: not significant.

Figure 5. LNP-DI290 inhibits DENV replication in infected IFNAR-deficient mice. (A) Schematic representation of the experimental design. IFNAR-deficient mice were *i.p.* infected with mouse-adapted DENV-2 strain D220 (10^4 $CCID_{50}$ per mouse). After 4 h infection, the mice were *i.p.* treated with either empty LNP or LNP-DI290 (15 µg DI290 RNA per mouse). (B and C) Viremia and virus titers in spleen were measured by $CCID_{50}$ assay at 72 h post-infection (n=6). (D) The level of DENV-2 D220 RNA in spleen was measured by RT-qPCR using primers for the D220 NS5 region (n=6). (E) The percentage of weight change was monitored at 72 h post-infection (n=6). Data are shown as the mean ± standard error of mean (SEM). Two-tailed Student's t test and Kolmogorov-Smirnov test were used for statistical analysis. L.D.: limit of detection. ns: not significant.

Figure 6. LNP-DI290 block DENV replication in infected IRF3/IRF7 DKO mice. (A) Schematic representation of the experimental design. IRF3/IRF7 DKO mice were *i.p*. infected with D220 (10^4 $CCID_{50}$ per mouse). After 4 h infection, the mice were *i.p.* treated with either empty LNP or LNP-DI290 (15 µg DI290 RNA per mouse). (B and C) Viremia and virus titres in spleen were measured by $CCID_{50}$ assay at 72 h post-infection (n=6). (D) The level of D220 DENV-2 RNA in spleen was measured by RT-qPCR using primers for the D220 NS5 region (n=6). (E) The percentage of weight change was monitored for at 72 h post-infection (n=6). Data are shown as the mean ± SEM. Two-tailed Student's *t* test was used for statistical analysis. L.D.: limit of detection. ns: not significant.

Figure 7 Results of EdgeR analysis. Heatmap shows log_2 fold-changes of 87 DEGs that were significantly upregulated in all four experimental groups. DEGs are ordered by log_2 fold-change in the LNP-DI290 treated MDM (MDM_LNP-DI290) group.

Figure 8: Results of IPA Core Analysis. (A) Heatmap shows activation z-scores of 117 cytokine/chemokine USRs that displayed significant activation or inhibition in at least one experimental group. Any USR that was not significant in a particular group was given a z-score of zero. USRs are ordered by z-score in the MDM group treated with LNP290 (MDM_LNP-DI290). (B) Heatmap shows activation z-scores of transcription factor USRs that displayed significant activation or inhibition in at least one experimental group. The 100 most activated/inhibited USRs across all groups are shown. Any USR that was not significant in a particular group was given a z-score of zero. USRs are ordered by z-score in the MDM_LNP-DI290 group.

Fig.1

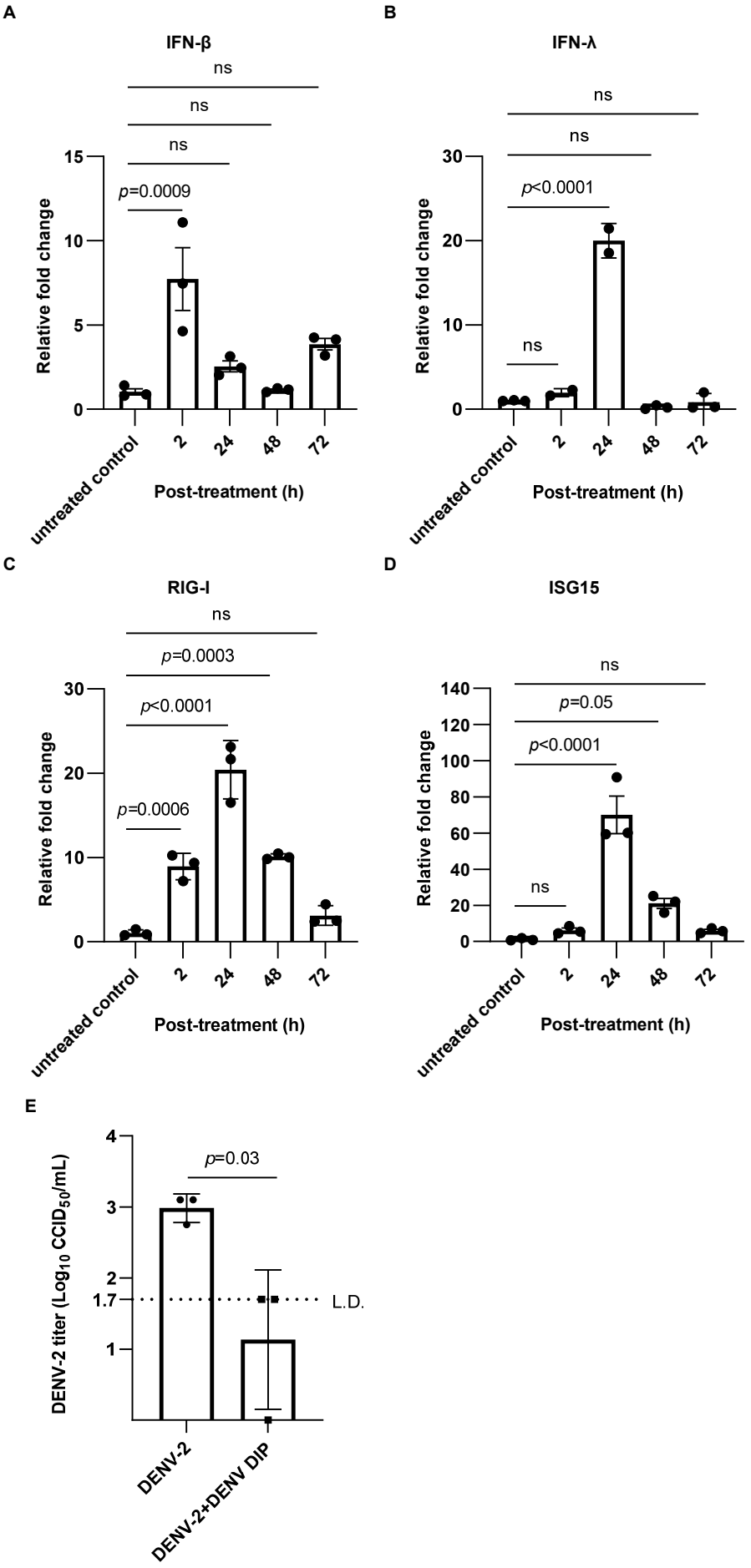
A
IFN-β
ns
ns
ns
p=0.0009
Relative fold change
15
10
5
0
untreated control
2
24
48
72
Post-treatment (h)
B
IFN-λ
ns
ns
p<0.0001
ns
Relative fold change
30
20
10
0
untreated control
2
24
48
72
Post-treatment (h)
C
RIG-I
ns
p=0.0003
p<0.0001
p=0.0006
Relative fold change
30
20
10
0
untreated control
2
24
48
72
Post-treatment (h)
D
ISG15
ns
p=0.05
p<0.0001
ns
Relative fold change
140
120
100
80
60
40
20
0
untreated control
2
24
48
72
Post-treatment (h)
E
p=0.03
DENV-2 titer (Log10 CCID50/mL)
4
3
2
1.7
1
L.D.
DENV-2
DENV-2+DENV DIP

Fig.2

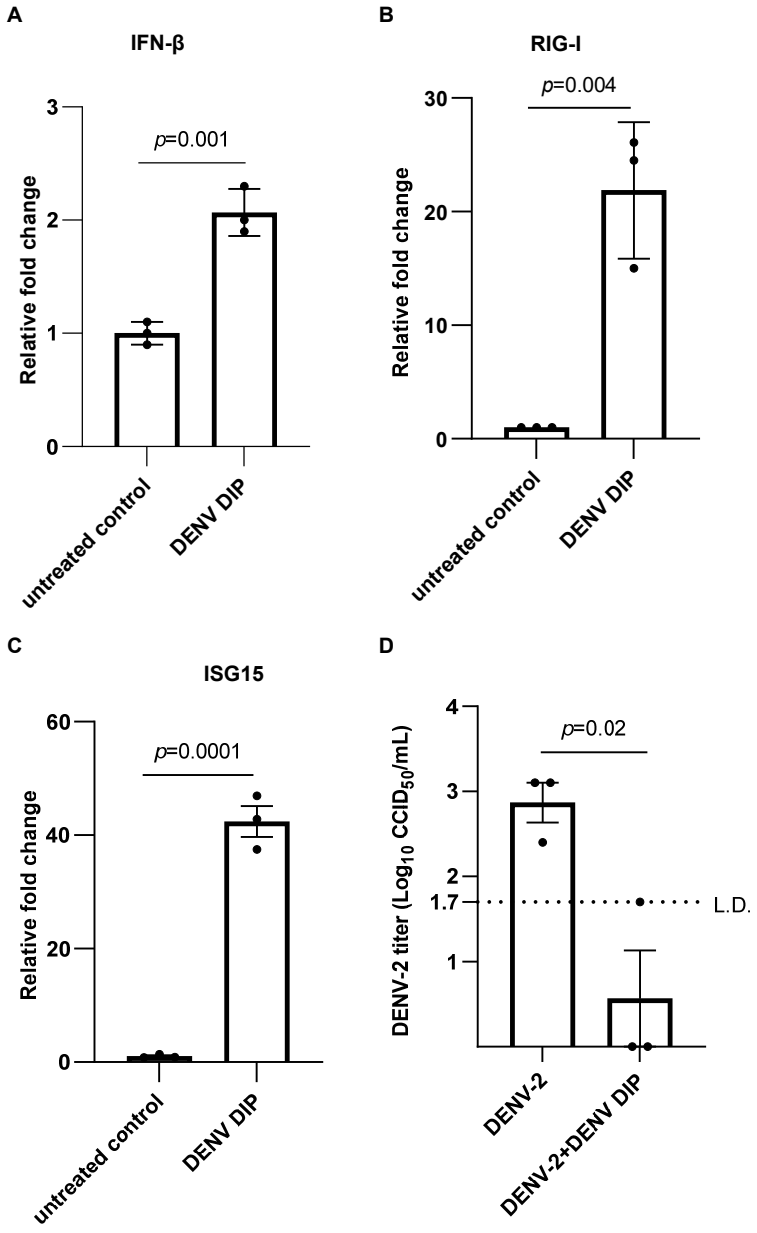
A
IFN-β
p=0.001
Relative fold change
3
2
1
0
untreated control
DENV DIP
B
RIG-I
p=0.004
Relative fold change
30
20
10
0
untreated control
DENV DIP
C
ISG15
p=0.0001
Relative fold change
60
40
20
0
untreated control
DENV DIP
D
p=0.02
DENV-2 titer (Log10 CCID50/mL)
4
3
2
1.7
1
L.D.
DENV-2
DENV-2+DENV DIP

Fig.3

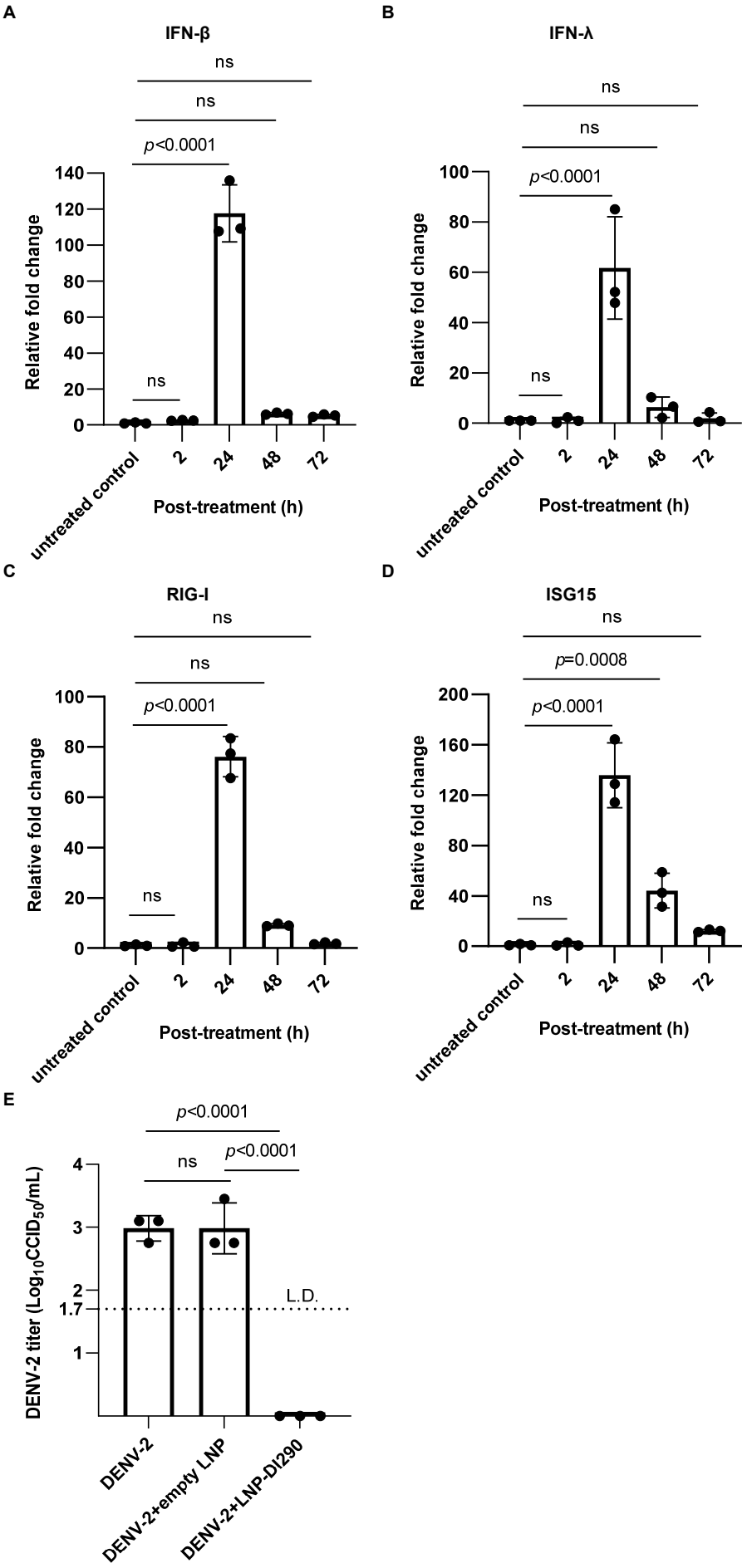
A
IFN-β
ns
ns
p<0.0001
ns
Relative fold change
140
120
100
80
60
40
20
0
untreated control
2
24
48
72
Post-treatment (h)
B
IFN-λ
ns
ns
p<0.0001
ns
Relative fold change
100
80
60
40
20
0
untreated control
2
24
48
72
Post-treatment (h)
C
RIG-I
ns
ns
p<0.0001
ns
Relative fold change
100
80
60
40
20
0
untreated control
2
24
48
72
Post-treatment (h)
D
ISG15
ns
p=0.0008
p<0.0001
ns
Relative fold change
200
160
120
80
40
0
untreated control
2
24
48
72
Post-treatment (h)
E
p<0.0001
ns
p<0.0001
DENV-2 titer (Log10CCID50/mL)
4
3
2
1.7
1
L.D.
DENV-2
DENV-2+empty LNP
DENV-2+LNP-DI290

Fig.4

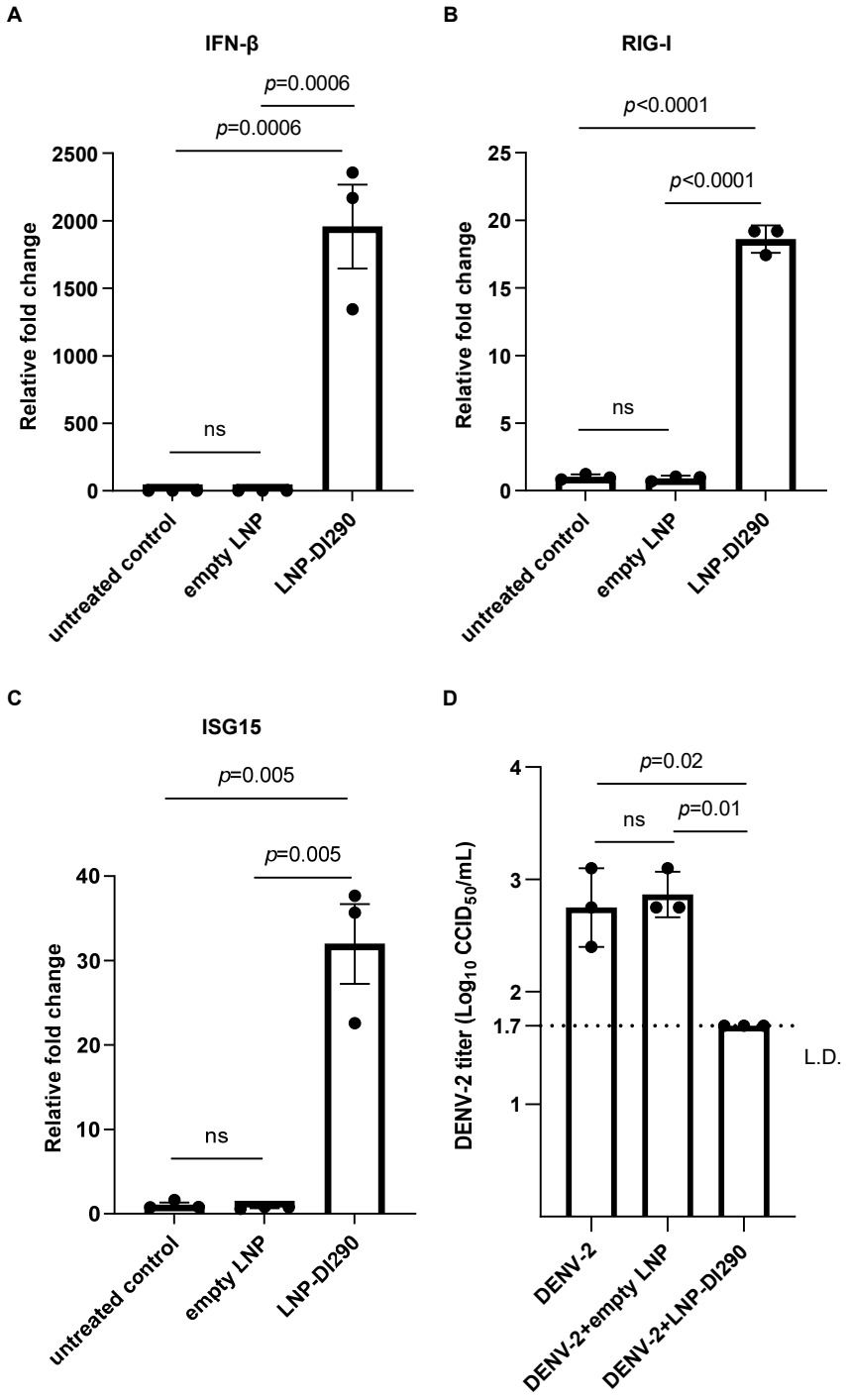
A
IFN-β
p=0.0006
p=0.0006
ns
Relative fold change
2500
2000
1500
1000
500
0
untreated control
empty LNP
LNP-DI290
B
RIG-I
p<0.0001
p<0.0001
ns
Relative fold change
25
20
15
10
5
0
untreated control
empty LNP
LNP-DI290
C
ISG15
p=0.005
p=0.005
ns
Relative fold change
40
30
20
10
0
untreated control
empty LNP
LNP-DI290
D
p=0.02
ns
p=0.01
DENV-2 titer (Log10 CCID50/mL)
4
3
2
1.7
1
L.D.
DENV-2
DENV-2+empty LNP
DENV-2+LNP-DI290

Fig.5

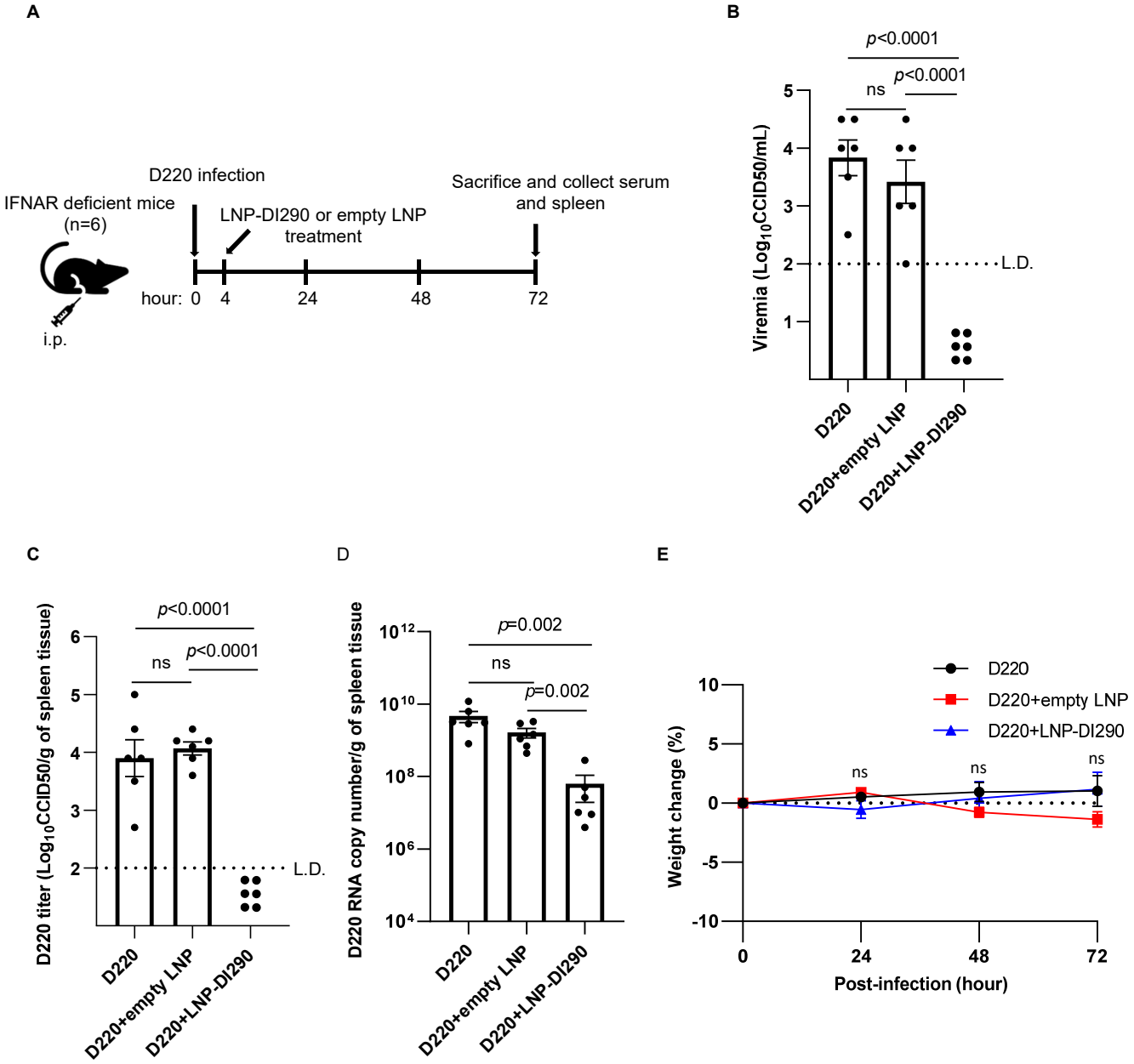
A
IFNAR deficient mice
(n=6)
i.p.
D220 infection
LNP-DI290 or empty LNP
treatment
Sacrifice and collect serum
and spleen
hour: 0 4 24 48 72
B
p<0.0001
p<0.0001
ns
Viremia (Log10CCID50/mL)
L.D.
D220
D220+empty LNP
D220+LNP-DI290
C
p<0.0001
p<0.0001
ns
D220 titer (Log10CCID50/g of spleen tissue)
L.D.
D220
D220+empty LNP
D220+LNP-DI290
D
p=0.002
p=0.002
ns
D220 RNA copy number/g of spleen tissue
D220
D220+empty LNP
D220+LNP-DI290
E
D220
D220+empty LNP
D220+LNP-DI290
ns
ns
ns
Weight change (%)
Post-infection (hour)

Fig.6

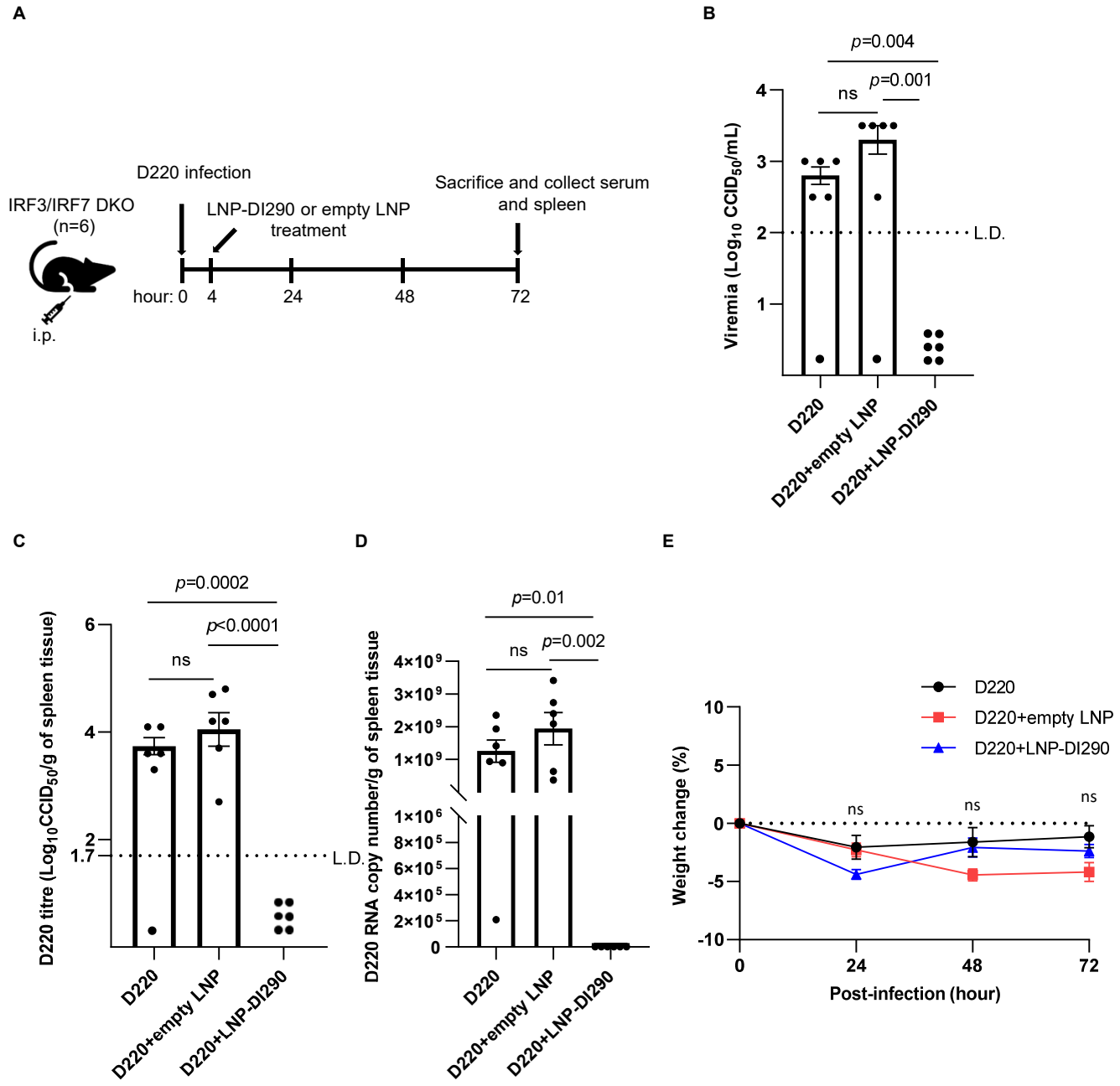
A
IRF3/IRF7 DKO
(n=6)
i.p.
D220 infection
LNP-DI290 or empty LNP
treatment
Sacrifice and collect serum
and spleen
hour: 0
4
24
48
72
B
p=0.004
ns
p=0.001
Viremia (Log10 CCID50/mL)
L.D.
D220
D220+empty LNP
D220+LNP-DI290
C
p=0.0002
p<0.0001
ns
D220 titre (Log10CCID50/g of spleen tissue)
L.D.
D220
D220+empty LNP
D220+LNP-DI290
D
p=0.01
ns
p=0.002
D220 RNA copy number/g of spleen tissue
D220
D220+empty LNP
D220+LNP-DI290
E
D220
D220+empty LNP
D220+LNP-DI290
Weight change (%)
ns
ns
ns
Post-infection (hour)

Fig.7

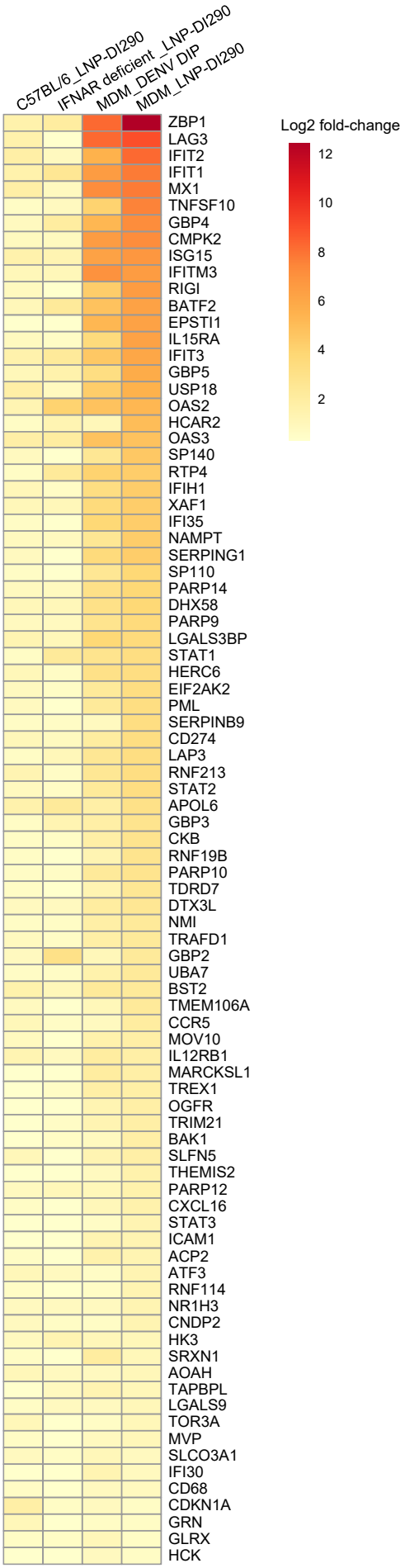
C57BL/6_LNP-DI290
IFNAR deficient _LNP-DI290
MDM_DENV DIP
MDM_LNP-DI290
ZBP1
LAG3
IFIT2
IFIT1
MX1
TNFSF10
GBP4
CMPK2
ISG15
IFITM3
RIGI
BATF2
EPSTI1
IL15RA
IFIT3
GBP5
USP18
OAS2
HCAR2
OAS3
SP140
RTP4
IFIH1
XAF1
IFI35
NAMPT
SERPING1
SP110
PARP14
DHX58
PARP9
LGALS3BP
STAT1
HERC6
EIF2AK2
PML
SERPINB9
CD274
LAP3
RNF213
STAT2
APOL6
GBP3
CKB
RNF19B
PARP10
TDRD7
DTX3L
NMI
TRAFD1
GBP2
UBA7
BST2
TMEM106A
CCR5
MOV10
IL12RB1
MARCKSL1
TREX1
OGFR
TRIM21
BAK1
SLFN5
THEMIS2
PARP12
CXCL16
STAT3
ICAM1
ACP2
ATF3
RNF114
NR1H3
CNDP2
HK3
SRXN1
AOAH
TAPBPL
LGALS9
TOR3A
MVP
SLCO3A1
IFI30
CD68
CDKN1A
GRN
GLRX
HCK
Log2 fold-change
12
10
8
6
4
2

Fig.8

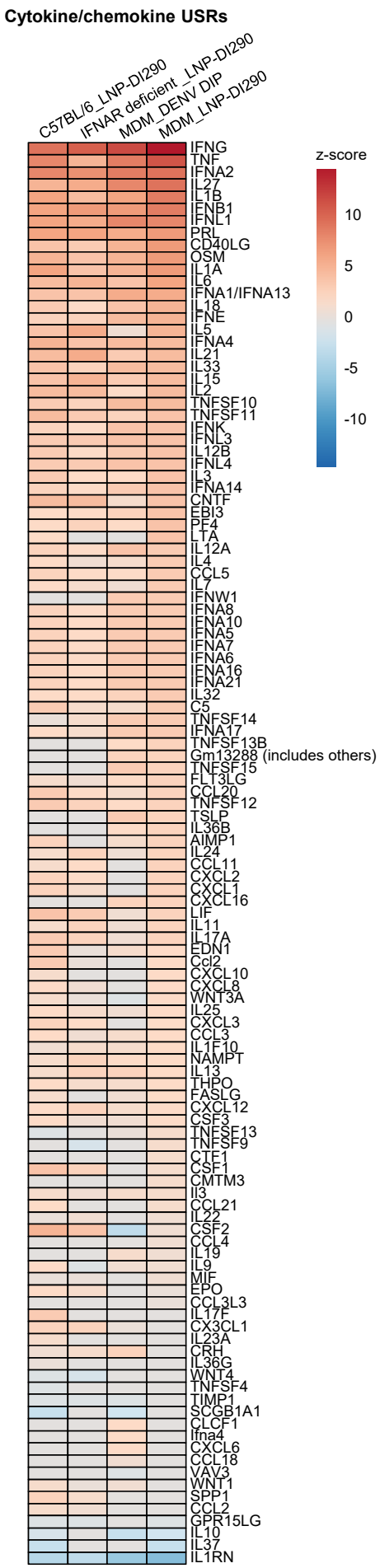
Cytokine/chemokine USRs
C57BL/6_LNP-DI290
IFNAR deficient _LNP-DI290
MDM_DENV DIP
MDM_LNP-DI290
z-score
10
5
0
-5
-10
IFNG
TNF
IFNA2
IL27
IL1B
IFNB1
IFNL1
PRL
CD40LG
OSM
IL1A
IL6
IFNA1/IFNA13
IL18
IFNE
IL5
IFNA4
IL21
IL33
IL15
IL2
TNFSF10
TNFSF11
IFNK
IFNL3
IL12B
IFNL4
IL3
IFNA14
CNTF
EBI3
PF4
LTA
IL12A
IL4
CCL5
IL7
IFNW1
IFNA8
IFNA10
IFNA5
IFNA7
IFNA6
IFNA16
IFNA21
IL32
C5
TNFSF14
IFNA17
TNFSF13B
Gm13288 (includes others)
TNFSF15
FLT3LG
CCL20
TNFSF12
TSLP
IL36B
AIMP1
IL24
CCL11
CXCL2
CXCL1
CXCL16
LIF
IL11
IL17A
EDN1
Ccl2
CXCL10
CXCL8
WNT3A
IL25
CXCL3
CCL3
IL1F10
NAMPT
IL13
THPO
FASLG
CXCL12
CSF3
TNFSF13
TNFSF9
CTF1
CSF1
CMTM3
Il3
CCL21
IL22
CSF2
CCL4
IL19
IL9
MIF
EPO
CCL3L3
IL17F
CX3CL1
IL23A
CRH
IL36G
WNT4
TNFSF4
TIMP1
SCGB1A1
CLCF1
Ifna4
CXCL6
CCL18
VAV3
WNT1
SPP1
CCL2
GPR15LG
IL10
IL37
IL1RN

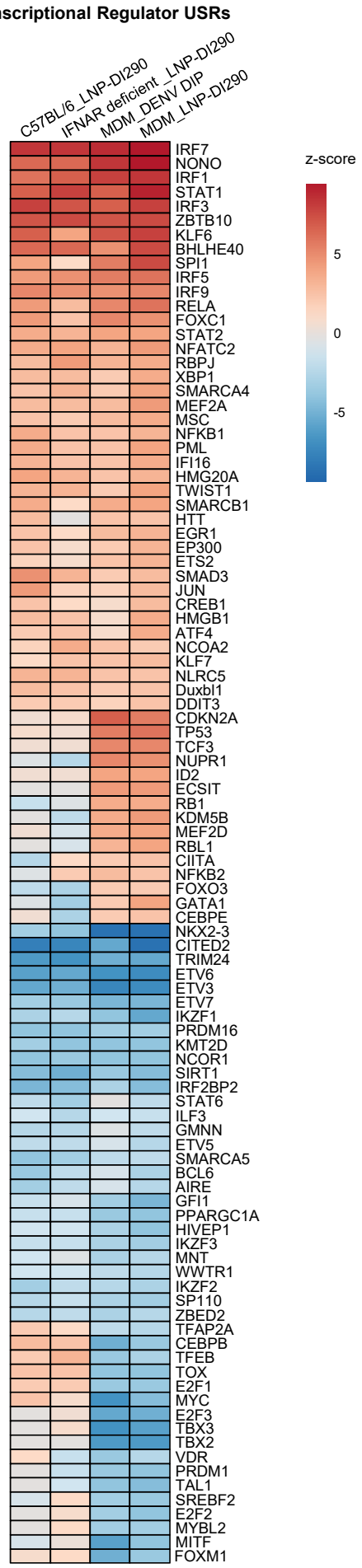
Transcriptional Regulator USRs
C57BL/6_LNP-DI290
IFNAR deficient _LNP-DI290
MDM_DENV DIP
MDM_LNP-DI290
z-score
5
0
-5
IRF7
NONO
IRF1
STAT1
IRF3
ZBTB10
KLF6
BHLHE40
SPI1
IRF5
IRF9
RELA
FOXC1
STAT2
NFATC2
RBPJ
XBP1
SMARCA4
MEF2A
MSC
NFKB1
PML
IFI16
HMG20A
TWIST1
SMARCB1
HTT
EGR1
EP300
ETS2
SMAD3
JUN
CREB1
HMGB1
ATF4
NCOA2
KLF7
NLRC5
Duxbl1
DDIT3
CDKN2A
TP53
TCF3
NUPR1
ID2
ECSIT
RB1
KDM5B
MEF2D
RBL1
CIITA
NFKB2
FOXO3
GATA1
CEBPE
NKX2-3
CITED2
TRIM24
ETV6
ETV3
ETV7
IKZF1
PRDM16
KMT2D
NCOR1
SIRT1
IRF2BP2
STAT6
ILF3
GMNN
ETV5
SMARCA5
BCL6
AIRE
GFI1
PPARGC1A
HIVEP1
IKZF3
MNT
WWTR1
IKZF2
SP110
ZBED2
TFAP2A
CEBPB
TFEB
TOX
E2F1
MYC
E2F3
TBX3
TBX2
VDR
PRDM1
TAL1
SREBF2
E2F2
MYBL2
MITF
FOXM1